

Supplemental material

Otani et al., <https://doi.org/10.1083/jcb.201812157>

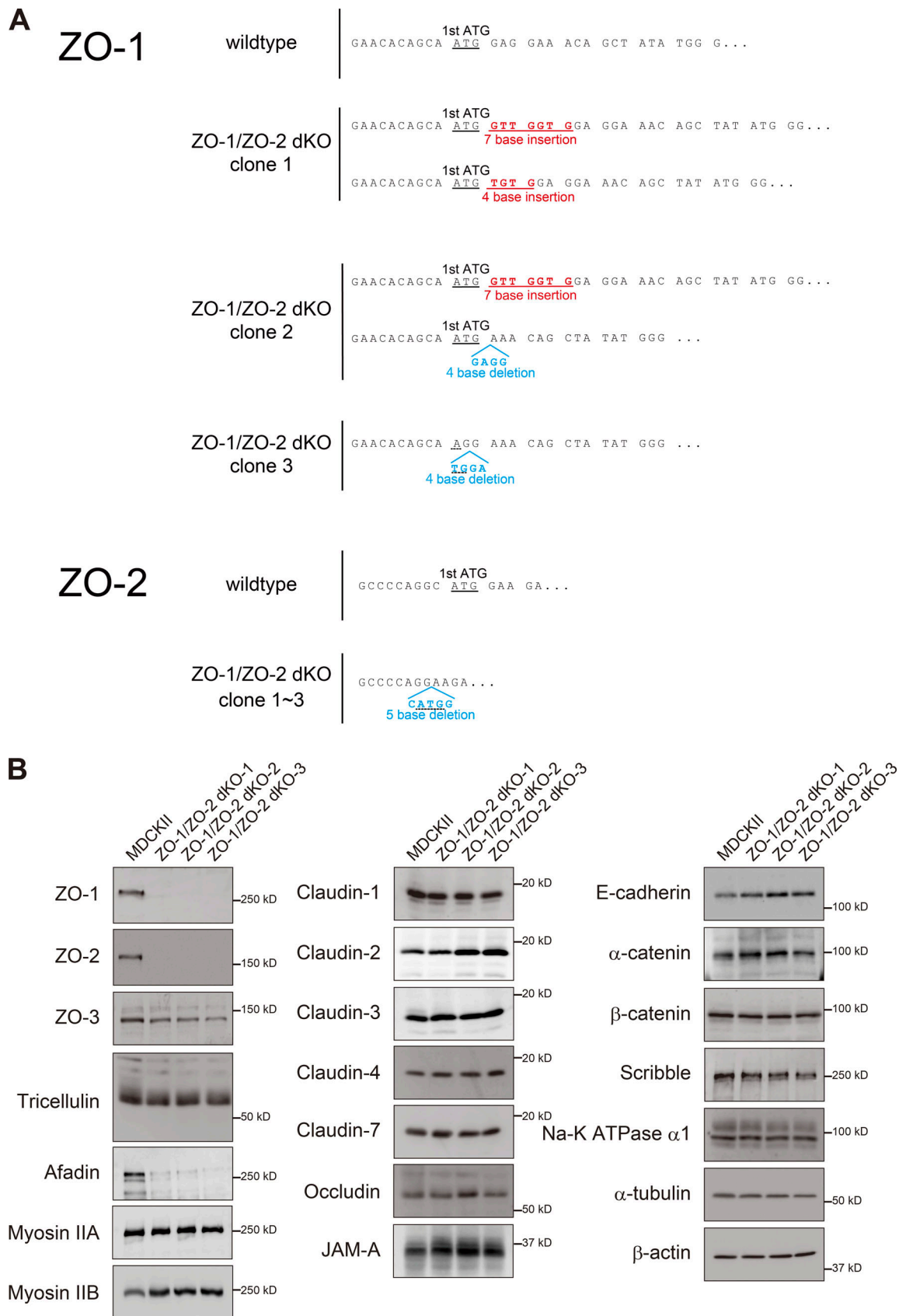


Figure S1. **Characterization of ZO-1/ZO-2 dKO cells.** (A) Genomic sequence of ZO-1/ZO-2 dKO cells. Frameshift mutations in ZO-1 and ZO-2 are found. (B) Western blotting analyses of ZO-1/ZO-2 dKO cells. Expression of ZO-1 and ZO-2 was abolished. Afadin expression was reduced in ZO-1/ZO-2 dKO cells. The expression levels of other proteins examined were not greatly altered.

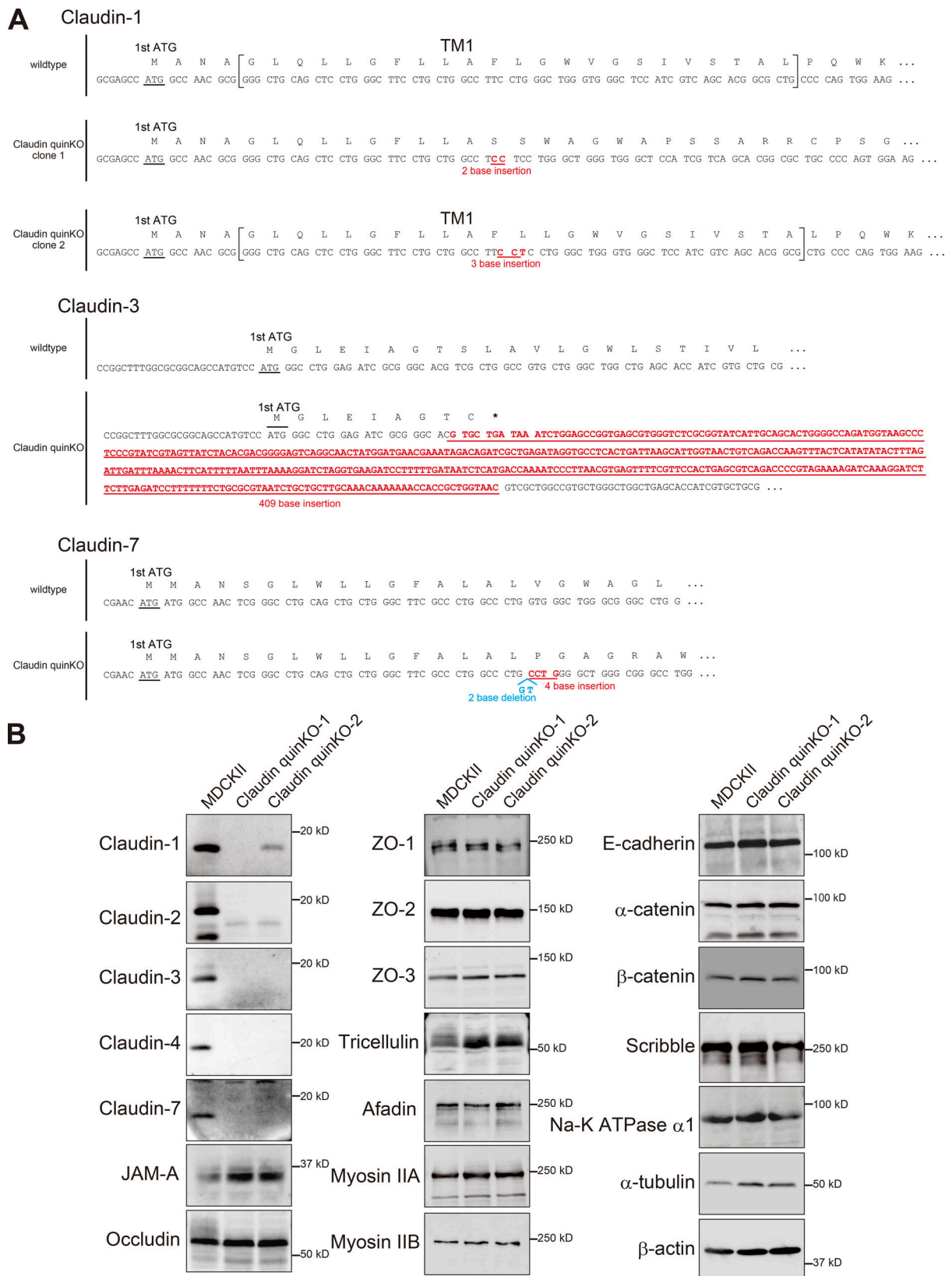


Figure S2. **Sanger sequencing of claudin quinKO cells. (A)** Genomic sequence of claudin quinKO cells revealed frameshift mutations in claudin-1, claudin-3, and claudin-7 in clone 1. In clone 2, a single amino acid insertion was found in the first transmembrane region of claudin-1 (TM1), resulting in intracellular accumulation and degradation of claudin-1. **(B)** Western blotting analyses of claudin quinKO cells. Expression of claudins was abolished in clone 1. Claudin-1 was degraded and reduced, and expression of claudin-2, claudin-3, claudin-4, and claudin-7 was abolished in clone 2. The expression levels of JAM-A and tricellulin were slightly increased in claudin quinKO cells. The expression levels of other proteins examined were not greatly altered.

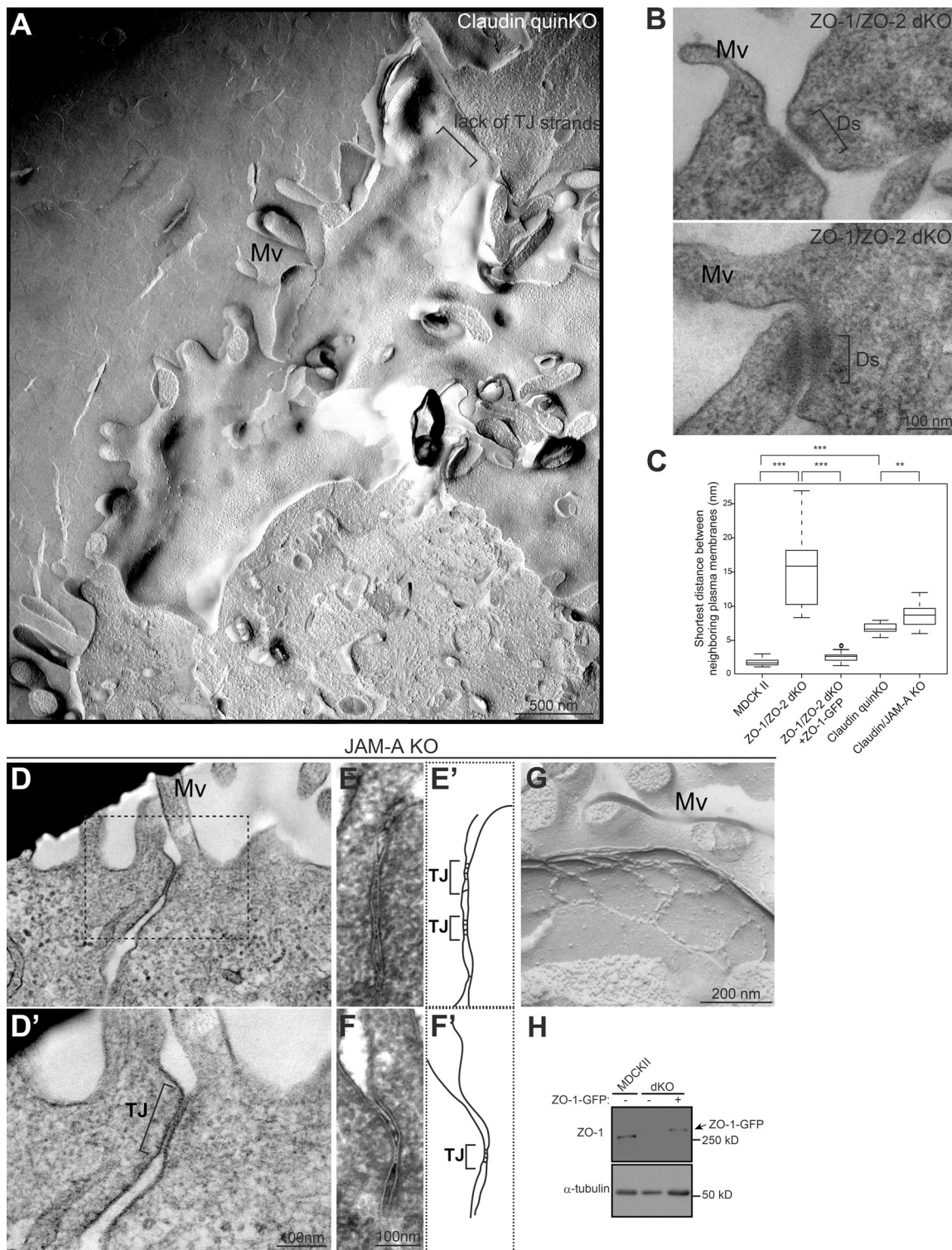


Figure S3. **Ultrastructural analyses of ZO-1/ZO-2 dKO, claudin quinKO, and JAM-A KO cells.** (A) Low-magnification view of a freeze-fracture replica from claudin quinKO cells. No TJ strands were found throughout the lateral plasma membrane, although some accumulation of intramembrane particles was occasionally observed. (B) Examples of ZO-1/ZO-2 dKO cells lacking AJs. Desmosomes (Ds) were found at the apical cell junctions, but no AJs were observed. (C) Quantification of the minimum distance between two plasma membranes. The relatively small difference between claudin quinKO and claudin/JAM-A KO cells is due to the remaining focal membrane appositions in claudin/JAM-A KO cells. Graphs represent mean \pm SD ($n = 13-29$). **, $P < 0.005$; ***, $P < 0.0005$, compared by t test. (D-G) Transmission EM analyses of JAM-A KO cells. (D) Typical TJ structures with tightly apposed neighboring plasma membranes are observed. Black square indicates the region shown in the high magnification image. (E and F) TJ membrane kissing points were observed in JAM-A KO cells after ferrocyanide-reduced osmium/tannic acid/osmium postfixation. The most apical cell junctions were observed. (E' and F') Tracing of TJs. (G) Freeze-fracture replica EM of JAM-A KO cells. TJ strand structures were formed beneath the apical microvilli in JAM-A KO cells. (H) Western blotting showed that ZO-1-GFP restored ZO-1 expression in ZO-1/ZO-2 dKO cells. Ds, desmosome; Mv, microvilli. Scale bars: 500 nm (A); 100 nm (B-E); 200 nm (G).

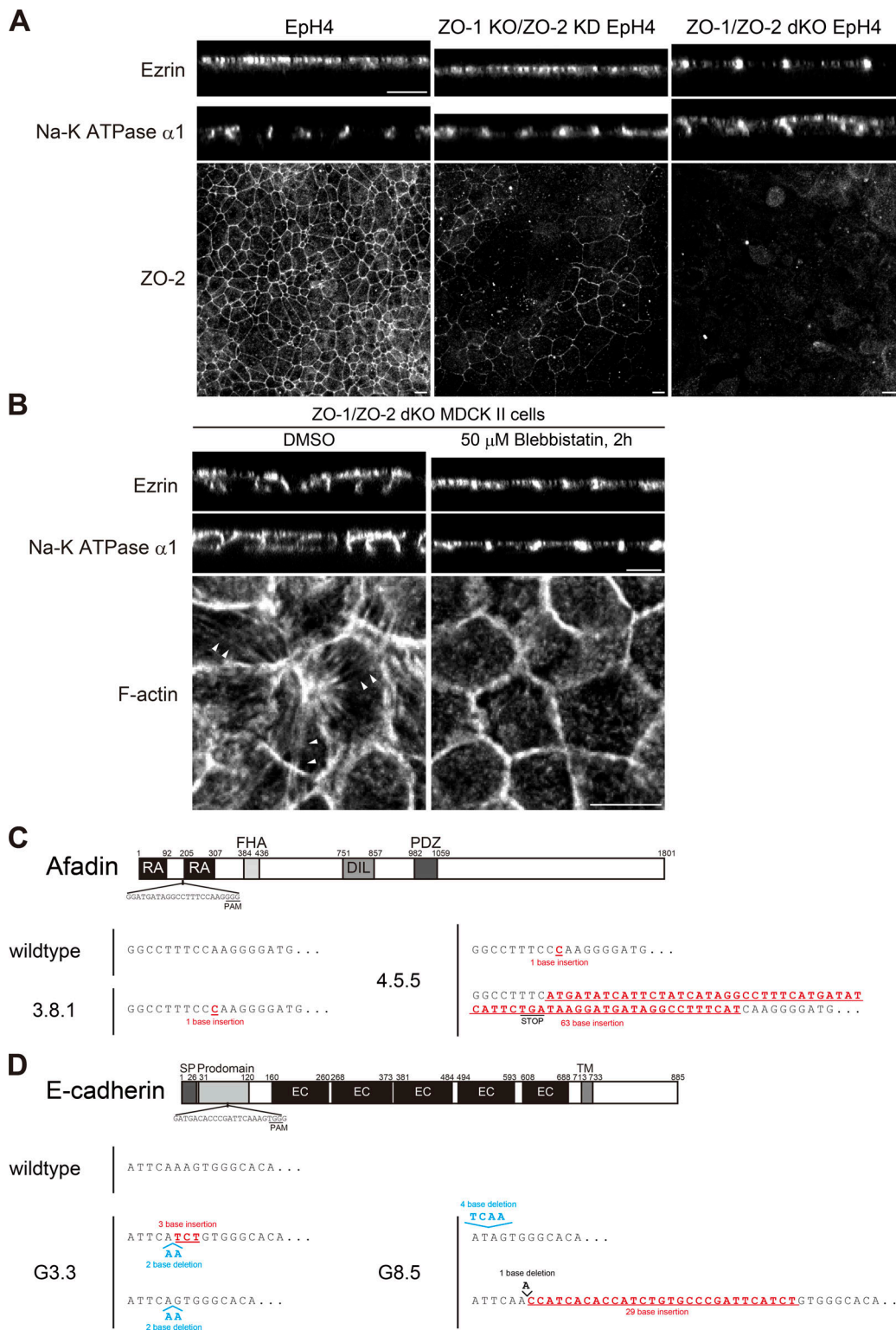


Figure S4. **ZO-1/ZO-2 regulate epithelial polarity independent of myosin II.** (A) Epithelial polarity was disorganized in ZO-1/ZO-2 dKO Eph4 cells. Ezrin was selectively localized to the apical membrane, while Na-K ATPase α1 subunit was restricted to the basolateral membrane in parental Eph4 cells and ZO-1 KO/ZO-2 KD Eph4 cells. In contrast, ezrin was mislocalized at the lateral cell contacts, Na-K ATPase α1 subunit was detected on both the apical and basolateral membranes in ZO-1/ZO-2 dKO Eph4 cells. ZO-2 staining shows that ZO-2 expression is completely lost in ZO-1/ZO-2 dKO Eph4 cells, whereas low but significant residual expression of ZO-2 is observed in ZO-1 KO/ZO-2 KD Eph4 cells at 5 d after plating. (B) Myosin II inhibition did not modify the epithelial polarity phenotypes. Treatment with myosin II inhibitor blebbistatin (50 μM, 2 h) did not modify the epithelial polarity phenotypes in ZO-1/ZO-2 dKO cells, although the cell height became shorter and the characteristic apical actin cables were lost upon blebbistatin treatment. Apical confocal sections are shown for F-actin staining. (C) Genomic sequences of Afadin KO cells. Frameshift or nonsense mutations are found. (D) Genomic sequences of E-cadherin KO cells. Frameshift mutations are found. Scale bars: 10 μm.

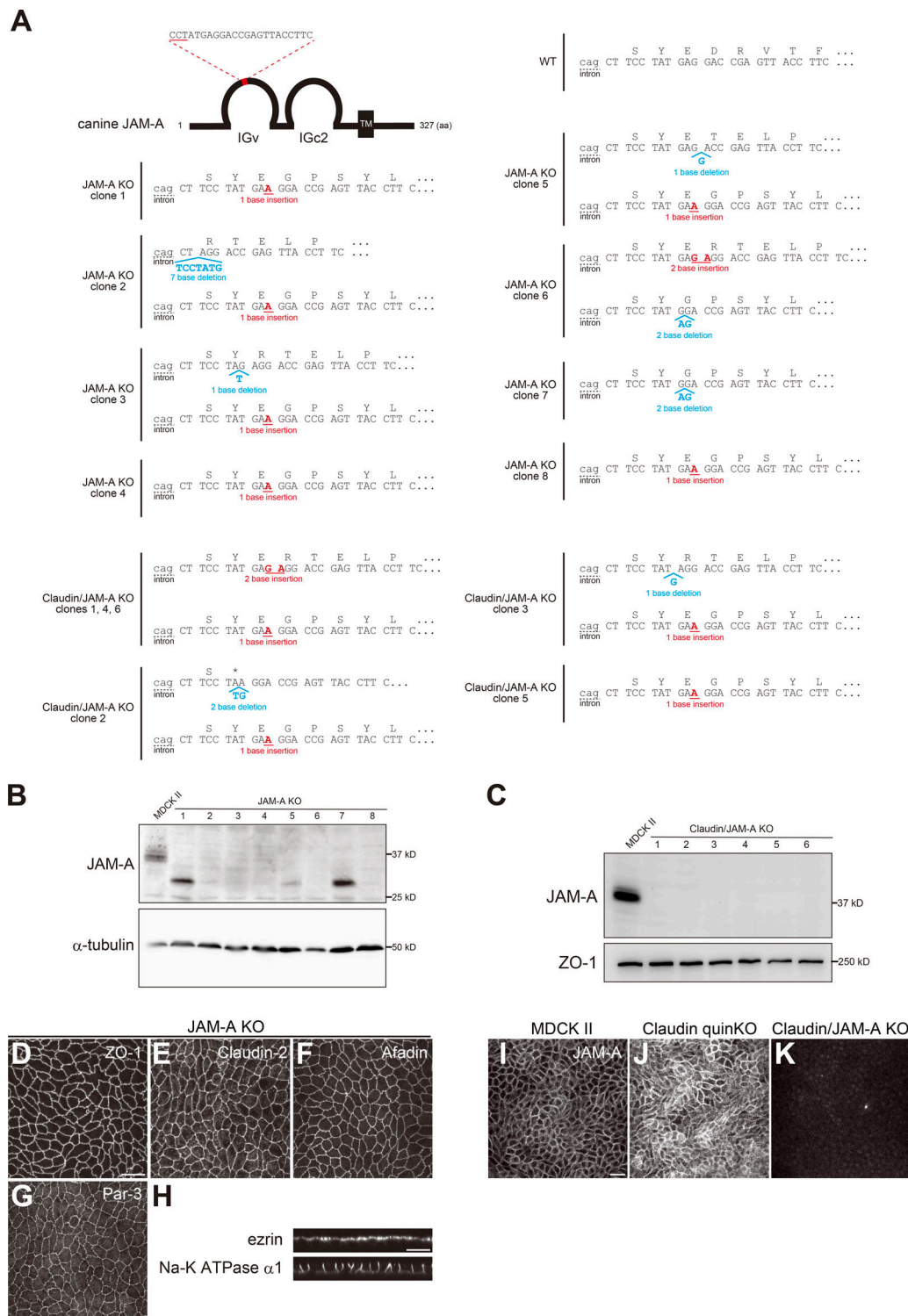


Figure S5. **Characterization of JAM-A KO and claudin/JAM-A KO cells.** (A) Genomic sequence of JAM-A KO and claudin/JAM-A KO cells revealed frameshift or nonsense mutations. (B) Western blotting of JAM-A KO cells. JAM-A full-length protein expression is lost in JAM-A KO cells. Note that truncated protein is found in JAM-A KO clones 1 and 7. Nevertheless, all clones showed loss of JAM-A from cell junctions, and phenotypic analyses did not show any significant difference, suggesting that all clones are loss of function mutations (see Fig. 10 V, for example). The nature of the truncated protein is unclear, as we were not able to detect the nature of these mutations by our genomic PCR primers. However, as the target region is in proximity of the intron–exon boundary, it is likely to affect the splice acceptor site, resulting in exon skipping. (C) Western blotting of claudin/JAM-A KO cells. JAM-A protein expression is lost in claudin/JAM-A KO cells. (D–G) Cell junction protein localization in JAM-A KO cells. The cell junction localization is not perturbed. (H) No epithelial polarity defects are observed in JAM-A KO cells. Ezrin is restricted to the apical membranes, while Na-K ATPase α 1 subunit was localized at basolateral membranes. See Figs. 1, 2, 6, and 9 for control images. (I–K) Immunofluorescence analyses of JAM-A in MDCK II cells, claudin quinKO cells, and claudin/JAM-A KO cells. JAM-A staining is abolished in claudin/JAM-A KO cells. Scale bars: 20 μ m.